Free Radical Research, January 2007; 41(1): 110–119

informa
healthcare

Identification of free radical species derived from caffeic acid and related polyphenols

YUKA MAEGAWA, KEIJI SUGINO, & HIROMU SAKURAI

Department of Analytical and Bioinorganic Chemistry, Kyoto Pharmaceutical University, Kyoto, Japan

Accepted by Professor M. Davies

(Received 14 April 2006; in revised form 2 August 2006)

Abstract
Polyphenols are widely distributed in various fruits, vegetables and seasonings. It is well known that they have several physiological effects due to their antioxidative activities. Their activities depend on structural characteristics that favour the formation of their corresponding stable radicals. During the examination at which pH values, the polyphenol radicals are stabilized, we confirmed that polyphenol radicals were stabilized in $NaHCO_3/Na_2CO_3$ buffer (pH 10) rather than in physiological pH region. Then, we measured electron spin resonance (ESR) spectra at pH 10 to examine the characteristics of free radical species derived from caffeic acid (CA) with an unsaturated side chain, dihydrocaffeic acid (DCA) with a saturated side chain, chlorogenic acid (ChA) and rosmarinic acid (RA). In analyzing the radical structures, ESR simulation, determinations of macroscopic and microscopic acid dissociation constants and molecular orbital (MO) calculation were performed. In CA, the monophenolate forms were assumed to participate in the formation of free radical species, while in DCA, the diphenol form and the monophenolate forms were presumed to contribute to the formation of free radical species. On the basis of the results, we propose the possible structures of the free radical species formed from polyphenols under alkaline conditions.

Keywords: *Polyphenol, free radical species, caffeic acid, ESR simulation, acid dissociation constant, molecular orbital calculation*

Introduction

In recent times, the effects of antioxidants on humans with respect to the maintenance of health, protection from certain diseases and the retardation of aging are of increasing interest to scientists [1–5].

It is well known that polyphenols exist as antioxidative components in some seeds, fruits and vegetables [6–10]. The main action mechanism of phenolic antioxidants is considered to be the scavenging or quenching of free radicals and reactive oxygen species (ROS), although other mechanisms may also be involved [11]. The radical scavenging activity of polyphenols depends on the structural characteristics that favour phenolic hydrogen donation and the stability of the resulting phenoxyl radicals [12].

However, little is known about the actual forms of the free radical species derived from polyphenols. Thus, we conducted a series of trials to analyse and identify the free radical species derived from polyphenols. In this study, we selected caffeic acid (CA) and chlorogenic acid (ChA), which are typical polyphenols found in foods such as sunflower seeds [13], potatoes [14] and coffee beans [15]. Studies on structure–activity relationships have revealed the contribution of the catechol moiety present in CA derivatives to their free radical scavenging activities [11,12,16]. However, the contribution of propenoic side chains to the radical scavenging properties of polyphenols remains controversial [12,17–19]. In order to investigate the role of the unsaturated side chain of CA in free radical formations, dihydrocaffeic

Correspondence: H. Sakurai, Department of Analytical and Bioinorganic Chemistry, Kyoto Pharmaceutical University, 5 Nakauchi-cho, Misasagi, Yamasina-ku, Kyoto 607-8414, Japan. Tel: 81 75 595 4629. Fax: 81 75 595 4753. E-mail: sakurai@mb.kyoto-phu.ac.jp

ISSN 1071-5762 print/ISSN 1029-2470 online
DOI: 10.1080/10715760600943892

acid (DCA)—containing a saturated side chain—and rosmarinic acid (RA)—containing both CA and DCA—were also examined. The structures of the polyphenols used in this study are shown in Figure 1, together with the element number. In Figure 1, ferulic acid (FA) and dihydroferulic acid (DFA) are also involved. These compounds were used to determine the microscopic acid dissociation constants (microconstants) of CA and DCA.

In a preliminary experiment, we observed that CA radicals are stabilized in $NaHCO_3/Na_2CO_3$ buffer (pH 10) rather than in physiological pH region, as shown in Figure 2. Thus, in this study for the first stage, the free radical species derived from the four polyphenols—CA, DCA, ChA and RA—were quantified in $NaHCO_3/Na_2CO_3$ buffer at pH 10 by electron spin resonance (ESR) and their structures were then analysed by ESR simulation, macro- and microconstants determination, and molecular orbital (MO) calculations. Several studies have previously reported on radical formation by polyphenols [20–26]. On the basis of our results and those of others [20–26], we propose not only the possible structures of free radical species that are derived under alkaline conditions from the four listed polyphenols, but also the importance of the side chain structure in these compounds.

Materials and methods

Materials

CA and FA were purchased from Wako Pure Chemical Industries (Osaka, Japan). ChA was obtained from Aldrich (Milwaukee, USA). RA was purchased from ICN Biochemicals Inc. (Aurora, USA). DCA and DFA were obtained from Avocado Research Chemicals (Heysham, England). All other chemicals were commercial products of the highest available grade.

ESR analysis of free radical species of caffeic acid and related compounds

The free radical species derived from CA, DCA, ChA and RA were generated in an alkaline solution. ESR

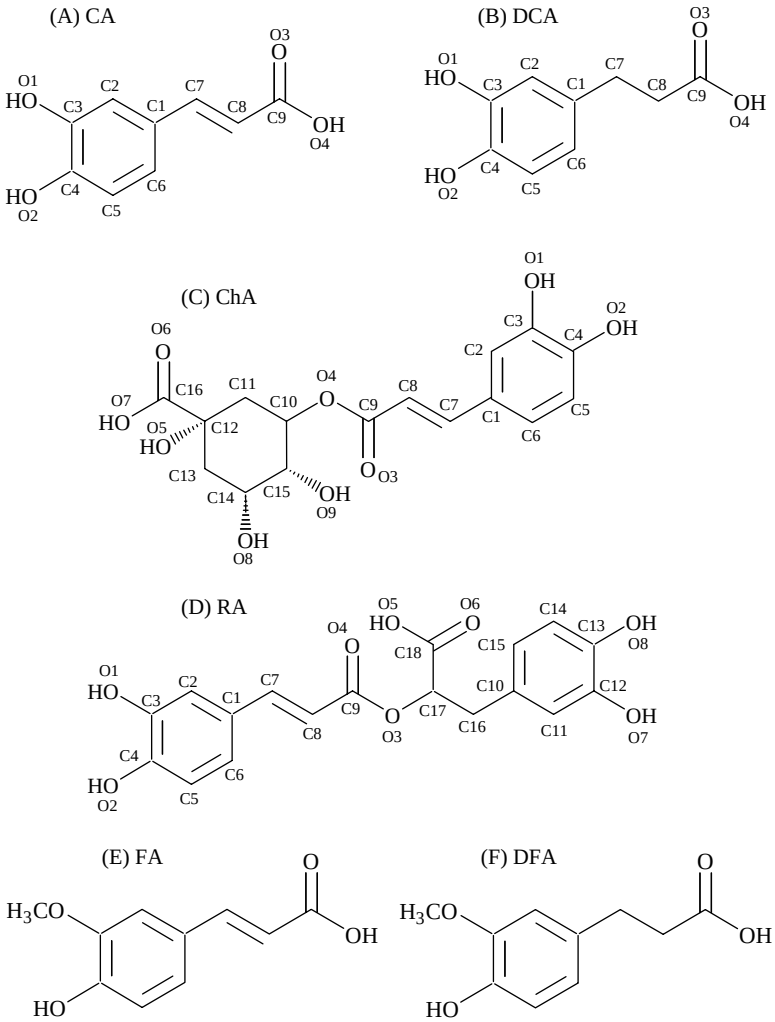

Figure 1. Chemical structures of (A) CA, (B) DCA, (C) ChA, (D) RA, (E) FA, and (F) DFA. The element numbers of CA, DCA, ChA and RA are also shown in the figure.

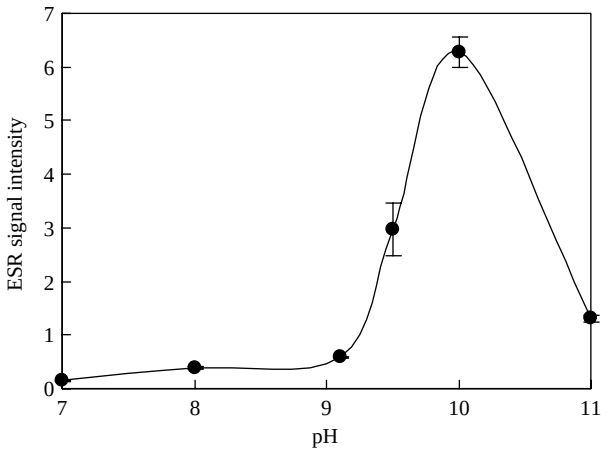

Figure 2. ESR signal intensities due to the CA radical depending on pH. CA was dissolved at a concentration of 5 mM in 0.1 M 2,4,6-trimethylpyridine–HCl buffer at pH 7.0 and 8.0 and in 0.1 M $NaHCO_3/Na_2CO_3$ buffer at pH 9.1, 9.5, 10.0 and 11.0. All spectra were measured 2 min after sample preparation. The data shown are the mean and standard deviation of the three experiments.

spectra were measured after 5 mM of CA, DCA, ChA and RA solutions were dissolved in 0.1 M $NaHCO_3/Na_2CO_3$ buffer (pH 10). The ESR spectra were recorded at room temperature by using an RFR-30 ESR spectrometer (JEOL, Tokyo, Japan) with a flat cell (Radical Research, Tokyo, Japan). The conditions under which the free radical species were detected were as follows: magnetic field = 335.0–339.5 ± 5 mT, power = 4 mW, modulation amplitude width = 0.1 mT, sweep time = 2 min, time constant = 0.03 s and gain = 160–500. Computer simulation for the free radical species was performed using WinRad ESR Data Analyzer ver. 1.20a (Radical Research, Tokyo, Japan).

In order to examine the relationship between the chemical species and the formation of the corresponding free radical species, the ESR spectra for the CA or DCA radical, which was detected in $NaHCO_3/Na_2CO_3$ buffer at pH 9.1, 9.5, 10.0 and 11.0 were measured. All spectra were measured 2 min after sample preparation. The CA and DCA samples were prepared at a concentration of 5 mM and 3.33 mM, respectively, which were the same concentrations used in the following potentiometric titration experiments.

Potentiometric titration and determination of the macroscopic and microscopic acid dissociation constants of the polyphenols

Using 20 ml of each sample solution, the macroscopic and microscopic acid dissociation constants (macro-constants and micro-constants, respectively) were determined by the potentiometric titration method. Titrations were carried out using a TIM 850 Titration Manager (Radiometer Analytical, Cedex, France). In all cases, the ionic strength was adjusted to 0.1 with $NaClO_4$ and the temperature was 25 ± 0.1°C. DCA and DFA were dissolved in water at concentrations of 3.33 mM. ChA and RA were dissolved in water at a concentration of 5 and 2.5 mM, respectively. Due to the poor water solubility of CA and FA, they were dissolved in mixed solvents that contained various ratios of acetonitrile and water; the concentration of both CA and FA was 5 mM. The acid dissociation constants in water were determined by extrapolation. The solution was stirred with a magnetic stirrer and nitrogen gas was gently passed into the solution during titration. The solution was titrated with carbonate-free standardized 0.1 M KOH [27]. The macro-constants of the compounds were calculated according to the titration method of Schwarzenbach [28] and the micro-constants of the compounds were calculated by the method of Edsall et al. [29–31].

Molecular orbital (MO) calculations

The MO calculations of CA, DCA, ChA and RA were performed using the MOPAC semi-empirical molecular orbital package program (ver. 7.0). MOPAC internal files were prepared using MOLDA, a molecular-model building program. Optimized geometrical structures that were obtained by using the PM3 Hamiltonian function were used to determine the MO energy of the highest occupied MO (HOMO) [32,33].

Results and discussion

ESR analysis of free radical species of caffeic acid and related compounds that were generated in an alkaline solution: Contribution of side chain

Preliminarily, we examined the optimal pH value for the generation of the free radical species of CA and we observed that $NaHCO_3/Na_2CO_3$ buffer at pH 10 was the most suitable condition (Figure 2). It is conceivable that the stabilization of these free radical species derived from polyphenols is specific to the carbonate buffer because we observed that the ESR signal intensities of CA radicals weakened more rapidly in NaOH solution than in carbonate buffer (Figure 3). Our results were supported by previous data that reported that of the solutions tested, carbonate buffer yielded the strongest signal of the ChA radical [34]. Thus, we used this buffer during the course of our study. The ESR spectra for CA, DCA, ChA and RA were detectable soon after these four compounds were dissolved in the carbonate buffer (Figure 4).

The ESR spectra for CA and ChA exhibited splitting and comprised seven signals. A similar type of spectrum was also reported for the ethyl caffeate radical that was formed in alkali solution by aeration [22]. It was also reported that identical ESR spectra due to two radical species were detected in strongly alkaline solutions of CA and ChA [25]. On the other hand, the spectra of DCA and RA exhibited splitting and comprised four signals. As shown in Figure 1,

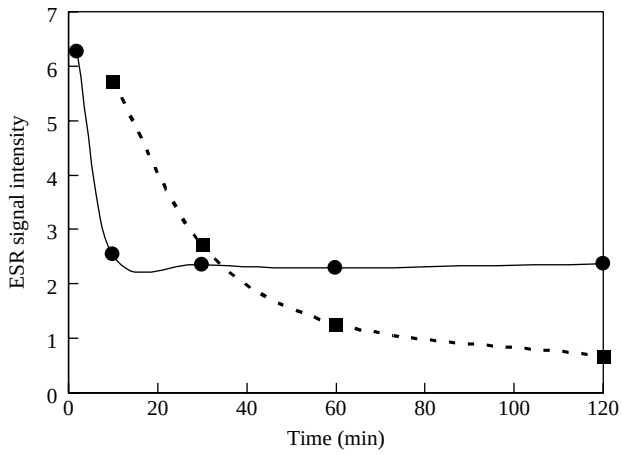

Figure 3. Time-dependent change in the ESR signal intensity due to the CA radical. CA was dissolved at a concentration of 5 mM in 0.1 M $NaHCO_3/Na_2CO_3$ buffer (pH 10) or in NaOH solution whose pH was adjusted to 10. The data shown are the mean of the duplicate experiments.

[in carbonate buffer in NaOH solution]

both CA and ChA have an unsaturated side chain, DCA has a saturated one and RA has both. This suggests that the appearance of different ESR spectral shapes is related to the chemical structure of the compounds.

An ESR simulation study of catechol and gallic acid was performed previously and it revealed that phenoxyl radicals were generated and that these radicals interconverted between limiting structures [23]. Thus, ESR simulation is considered to be useful in identifying the structures of the radicals. As shown in Table I, the results of ESR simulation showed that the hyperfine coupling constants (hfccs) of these spectra could be resolved; this was supported by the corresponding simulation spectra (Figure 4). The simulated spectra for CA and ChA revealed the presence of hyperfine coupling due to six inequivalent protons, while the spectra for RA and DCA revealed hyperfine coupling due to both five inequivalent protons and one pair of equivalent protons. These results indicate also that the CA and ChA radicals have a similar structure and that the RA and DCA radicals also have a similar structure. From these results, the appearance of different ESR spectral shapes is concluded to relate to the chemical structure of the compounds.

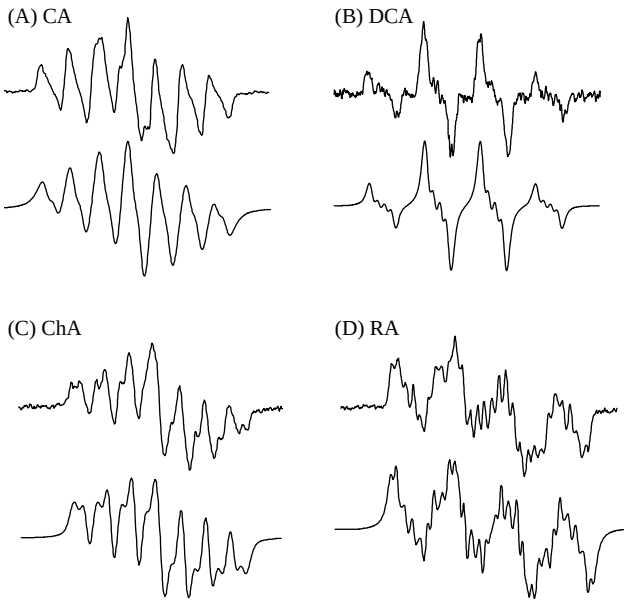

Figure 4. Observed and simulated ESR spectra of free radical species of (A) CA, (B) DCA, (C) ChA and (D) RA. CA, DCA, ChA and RA were dissolved in 0.1 M $NaHCO_3/Na_2CO_3$ buffer (pH 10) at a concentration of 5 mM. All spectra were measured 2 min after sample preparation. For each compound, the observed and simulated spectra are shown at the top and the bottom, respectively.

Potentiometric titration and determination of macro-scopic and micro-scopic acid dissociation constants of the polyphenols

Potentiometric titrations were performed to determine the most important chemical species in the formation of free radical species. CA and DCA were examined as a representative of the four compounds. CA and DCA dissociate in aqueous solution, as shown in Figure 5. Each chemical species is labelled as described in the figure. CA and DCA have three macro-constants (K_1, K_2 and K_3), four micro-constants (k_1, k_2, k_{12} and k_{21}) and a tautomeric constant (k_z). Micro-constants are related to macro-constants by the equations, as shown in Figure 5.

The macro- and micro-constants obtained for CA, FA, DCA and DFA are summarized in Table II along with reference data [18,35,36]. The macro-constants were calculated from the individual titration curves according to the method of Albert and Serjeant [27] and Schwarzenbach [29–31].

In general, when one macro-constant of a compound is substituted for one of the four micro-constants, the other three micro-constants can be determined by using the equations (1)–(4) in Figure 5 [29–31,37,38]. FA and DFA, which are derivatives of CA and DCA, respectively, were used in this study. Since protons dissociate from FA and DFA as shown in Figure 5, the macro-constant (K_2) of FA or DFA were expediently used as the values of the micro-constant (k_2) of CA or DCA.

As listed in Table III, the macro-constants of ChA and RA were also calculated from their titration curves. The p*K*a values of ChA, which has a partial structure of CA, were similar to those of CA. The pK_5 value of RA could not be calculated by the present method.

By using the obtained micro-constants of CA and DCA, the species distribution diagrams of CA and DCA were depicted as shown in Figure 6. The distribution ratios, which depend on the pH, for

Table I. The hyperfine coupling constants (mT) of CA, ChA, RA and DCA.

	a^{H}	a^{H}	a^{H}	a^{H}	a^{H}	a^{H}
CA	0.275(1)	0.245(1)	0.125(1)	0.115(1)	0.045(1)	0.022(1)
ChA	0.262(1)	0.242(1)	0.132(1)	0.118(1)	0.050(1)	0.045(1)
RA	0.370(1)	0.315(1)	0.205(1)	0.090(1)	0.045(1)	0.030(2)
DCA	0.368(1)	0.360(1)	0.355(1)	0.090(1)	0.045(1)	0.015(2)

The numbers shown in parentheses are the number of equivalent hydrogen atoms interacting with unpaired electron.

each chemical species are given by the following equations (5)–(9).

$$[\mathrm{H{\cdot}HAH}] = \frac{[\mathrm{H{\cdot}HAH}]}{[\mathrm{H{\cdot}HAH}] + [\mathrm{HAH}] + [\mathrm{HA}] + [\mathrm{AH}] + [\mathrm{A}]} = \frac{1}{1 + \frac{K_1}{[\mathrm{H^+}]} + \frac{K_1 k_2}{[\mathrm{H^+}]^2} + \frac{K_1 k_1}{[\mathrm{H^+}]^2} + \frac{K_1 k_1 k_{12}}{[\mathrm{H^+}]^3}} \quad (5)$$

Similarly,

$$[\mathrm{HAH}] = \frac{1}{\frac{[\mathrm{H^+}]}{K_1} + 1 + \frac{k_2}{[\mathrm{H^+}]} + \frac{k_1}{[\mathrm{H^+}]} + \frac{k_1 k_{12}}{[\mathrm{H^+}]^2}} \quad (6)$$

$$[\mathrm{HA}] = \frac{1}{\frac{[\mathrm{H^+}]^2}{K_1 k_2} + \frac{[\mathrm{H^+}]}{k_2} + 1 + k_z + \frac{k_{21}}{[\mathrm{H^+}]}} \quad (7)$$

$$[\mathrm{AH}] = \frac{1}{\frac{[\mathrm{H^+}]^2}{K_1 k_1} + \frac{[\mathrm{H^+}]}{k_1} + \frac{1}{k_z} + 1 + \frac{k_{12}}{[\mathrm{H^+}]}} \quad (8)$$

$$[\mathrm{A}] = \frac{1}{\frac{[\mathrm{H^+}]^3}{K_1 k_1 k_{12}} + \frac{[\mathrm{H^+}]^2}{k_1 k_{12}} + \frac{[\mathrm{H^+}]}{k_{21}} + \frac{[\mathrm{H^+}]}{k_{12}} + 1} \quad (9)$$

The diagrams show that both the monophenolate (HA) and (AH) forms participate in the formation of free radical species derived from CA, since the species distribution curves of the (HA) and (AH) forms correlate well with the changes in the ESR signal intensities due to the CA radicals. While, the diphenol (HAH) form as well as the monophenolate (HA) and (AH) forms appear to be involved in the formation of DCA radicals, in which a complicated distribution of free radical species is observed.

Molecular orbital calculations

Previously, pulse radiolysis, ESR spectroscopy and theoretical calculations for CA oligomer radicals were examined by comparing experimental results with theoretical results; the coupling constants of CA, DCA and RA obtained from ESR experiments and the density functional theory (DFT) calculations for these molecules correlated well [26]. We subsequently tried to carry out theoretical calculations in order to identify the structures of the free radical species of the four polyphenols.

The resulting optimized geometrical structures were obtained by using the PM3 Hamiltonian function for the major chemical species involved in free radical formation, i.e. (AH) and (HA) forms for CA, (HAH), (AH) and (HA) forms for DCA, (AH) and (HA) forms for ChA, and (HA–AH) and (HA–HA) forms for RA.

The HOMO eigenvalues that were calculated for the optimized structures of CA and DCA are listed in Table IV. In the (AH) form of CA, the C2, C4, C6 and

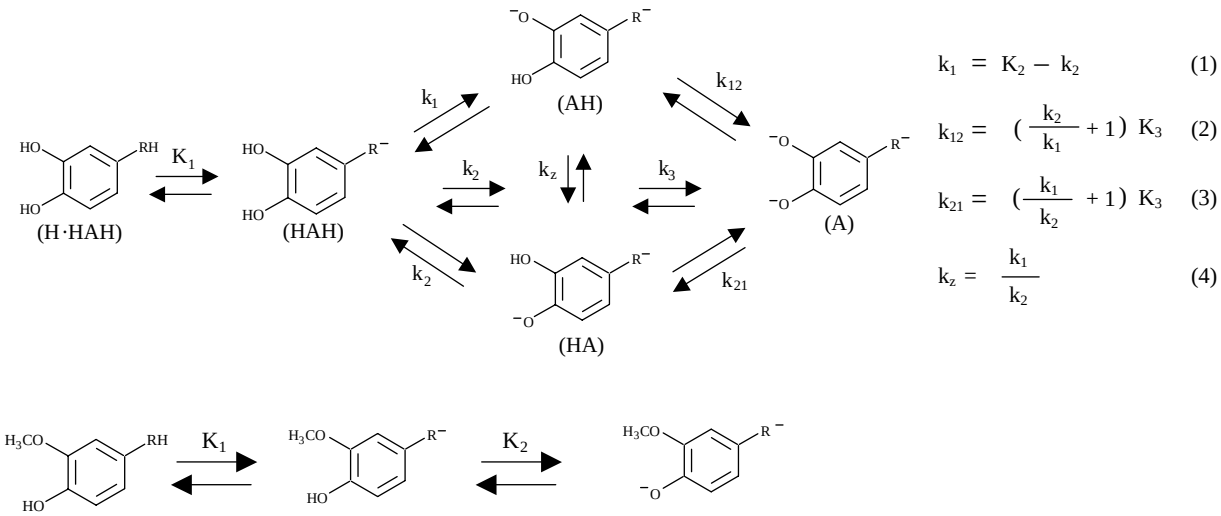

Figure 5. Acid dissociation equilibria for CA and DCA. The equilibria for FA and DFA are also shown at the bottom. For CA and FA, R: CH=CH–COO; for DCA and DFA, R: CH_2–CH_2–COO.

Table II. Macro- and microscopic acid dissociation constants of CA, FA, DCA and DFA.

	pK_1	pK_2	pK_3	pk_1	pk_2	pk_{12}	pk_{21}	k_z	
CA	4.43 ± 0.02	8.92 ± 0.03	11.12 ± 0.05	9.61 ± 0.10	9.03 ± 0.06	10.43 ± 0.17	11.01 ± 0.03	0.29 ± 0.09	This work*
	4.36 ± 0.03	8.48 ± 0.05	11.17 ± 0.30						Reference [18]
	4.37 ± 0.01	8.55 ± 0.01	12.5 ± 0.14						Reference [35]
	4.50	9.32	11.7						Reference [36]
FA	4.44 ± 0.03	9.03 ± 0.06							This work*
DCA	4.51 ± 0.03	9.52 ± 0.04	11.44 ± 0.03	9.65 ± 0.06	10.09 ± 0.01	11.30 ± 0.03	10.87 ± 0.08	2.79 ± 0.44	This work*
	4.43 ± 0.02	9.24 ± 0.02	11.38 ± 0.20						Reference [18]
DFA	4.59 ± 0.01	10.09 ± 0.01							This work*

* 25°C, $\mu = 0.1$ ($NaClO_4$), $n = 3$.

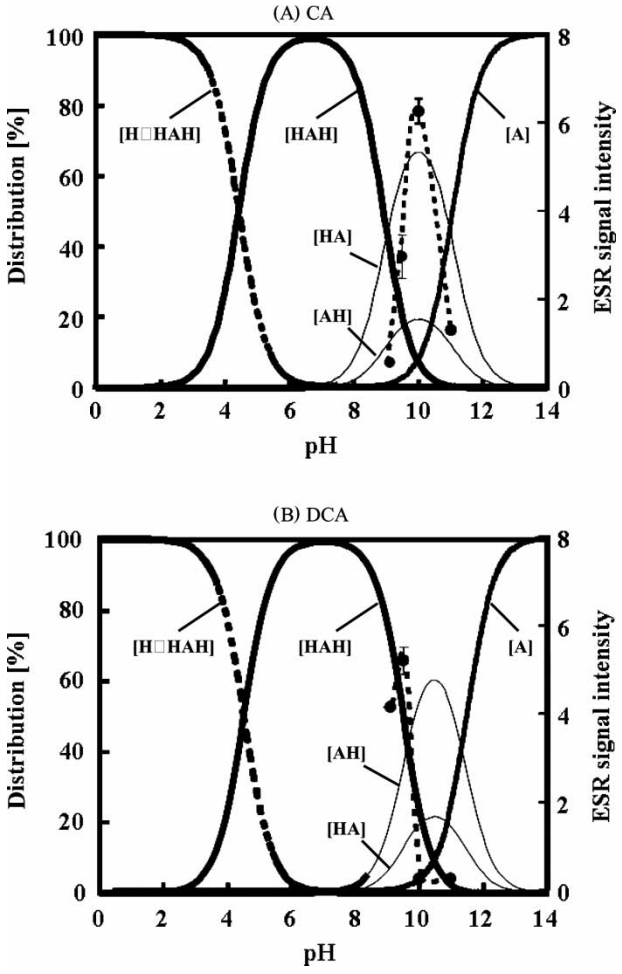

Figure 6. Species distribution diagrams of (A) CA, (B) DCA and their free radical species. Species distribution was determined from the calculated macro- and micro-constants. ESR spectra due to CA- or DCA-derived radicals were measured 2 min after sample preparation. CA and DCA were dissolved in 0.1 M $NaHCO_3/Na_2CO_3$ buffer at pH 9.1, 9.5, 10 and 11 at a concentration of 5 mM and 3.33 mM, respectively. The data shown are the mean and standard deviation of the three experiments.

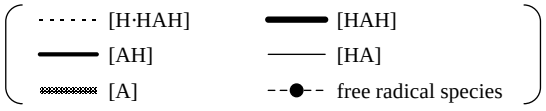

O1 atoms showed high HOMO values, while in the (HA) form, the C1, C3, C5, C8 and O2 atoms showed relatively high HOMO values, indicated by the bold typeface in the table. These atoms were presumed to form radicals because of their high electron-donating abilities. Thus, the free radical species derived from (AH) form and (HA) form have four and five resonance structures, respectively. The concept of resonance stabilization implies that in the case of CA, the radical species derived from the (HA) form would be more preferentially detected by ESR than the species derived from the (AH) form. The results obtained from the species distribution diagram of CA (Figure 6), in which (HA) radicals were formed

Table III. Macroscopic acid dissociation constants of ChA and RA.

	pK_1	pK_2	pK_3	pK_4	pK_5	
ChA	3.50 ± 0.04	8.42 ± 0.01	11.00 ± 0.02			This work*
	3.35 ± 0.02	8.21 ± 0.02	12.5 ± 0.15			Reference [35]
RA	2.92 ± 0.14	8.36 ± 0.08	9.56 ± 0.11	10.62 ± 0.16		This work*

* 25°C, $\mu = 0.1$ ($NaClO_4$), $n = 3$.

more preferentially than (AH) radicals, support the above assumption. Previously, the heat of formation values of CA semiquinoid radicals were calculated [21] and the results obtained were similar to ours.

In DCA, the O3 and O4 atoms of the (HAH) form, the C2, C4, C6 and O1 atoms of the (AH) form and the C1, C3, C5 and O2 atoms of the (HA) form showed high HOMO values. Taking resonance stabilization into consideration, the fact that both the (AH) and (HA) forms of DCA generate free radical species with four resonance structures leads to the assumption that the DCA radicals detected by ESR are the species formed from both the (AH) and (HA) forms. Since the species distribution diagram of DCA (Figure 6) indicates that (AH) radicals are formed more preferentially than (HA) radicals, in the case of DCA, the radical species derived from the (AH) form would be more preferentially detected by ESR than the radicals derived from the (HA) form. However, it does not make much difference for sensitivity of ESR detection between radicals derived from the (AH) form and those derived from the (HA) form in the case of CA, because the stabilities of the free radical species derived from the (AH) and (HA) forms are almost equivalent as for DCA. It is considered that the free radical species derived from the (HAH) form of DCA, which has only two resonance structures, cannot be detected due to their instability.

Similar results were obtained for ChA and RA, which are partial structures of CA and DCA, respectively (Table IV). Although RA has both a CA and DCA partial structure, the HOMO eigenvalues are localized in the DCA component. The results obtained from the MO calculations correlate well with

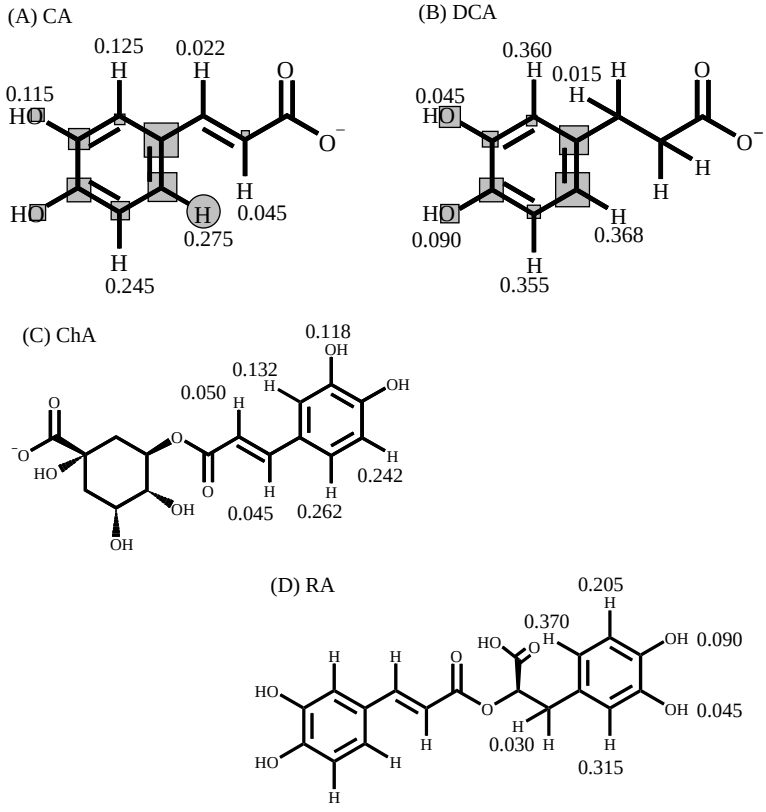

Figure 7. The assignment of hyperfine coupling constants for (A) CA, (B) DCA, (C) ChA and (D) RA. The radicalized regions in the resonance are assigned as the symbol ▨. The size of the symbol shows the easiness to be radicalized.

Table IV. HOMO electron densities of (A) CA, (B) DCA, (C) ChA and (D) RA (bold: relatively high HOMO values).

Element number	AH	HA	
(A)			
C1	0.023242	**0.494217**	
C2	**0.360061**	0.003378	
C3	0.084296	**0.367910**	
C4	**0.479416**	0.085698	
C5	0.000001	**0.344782**	
C6	**0.537892**	0.045602	
C7	0.001250	0.027660	
C8	0.008951	**0.203012**	
C9	0.000000	0.000001	
O1	**0.409332**	0.070613	
O2	0.094613	**0.338335**	
O3	0.000438	0.008765	
O4	0.000370	0.010054	
(B)	HAH	AH	HA
C1	0.000921	0.034972	**0.498179**
C2	0.000118	**0.353821**	0.000366
C3	0.000030	0.114358	**0.389881**
C4	0.000031	**0.443498**	0.122028
C5	0.000005	0.000017	**0.372408**
C6	0.000039	**0.523683**	0.059538
C7	0.001452	0.000890	0.005882
C8	0.022573	0.002090	0.024611
C9	0.001802	0.000186	0.001525
O1	0.000004	**0.429417**	0.085209
O2	0.000005	0.094701	**0.419768**
O3	**0.975771**	0.000624	0.004389
O4	**0.995519**	0.000399	0.004392
(C)	AH	HA	
C1	0.017365	**0.565292**	
C2	**0.412386**	0.007036	
C3	0.063573	**0.350662**	
C4	**0.472934**	0.047862	
C5	0.001065	**0.332538**	
C6	**0.534775**	0.012030	
C7	0.000019	0.004652	
C8	0.006009	**0.279727**	
C9	0.000210	0.011788	
C10	0.000001	0.000034	
C11	0.000004	0.000126	
C12	0.000001	0.000033	
C13	0.000000	0.000002	
C14	0.000000	0.000023	
C15	0.000003	0.000293	
C16	0.000000	0.000007	
O1	**0.407214**	0.083848	
O2	0.071515	**0.263246**	
O3	0.000602	0.034533	
O4	0.000115	0.005837	
O5	0.000000	0.000001	
O6	0.000000	0.000015	
O7	0.000001	0.000034	
O8	0.000000	0.000002	
O9	0.000000	0.000014	
(D)	HA–AH	HA–HA	
C1	0.000002	0.000027	
C2	0.000000	0.000003	
C3	0.000001	0.000016	
C4	0.000000	0.000006	
C5	0.000001	0.000016	
C6	0.000000	0.000007	
C7	0.000002	0.000044	
C8	0.000005	0.000029	
C9	0.000013	0.000158	
C10	0.045015	**0.516605**	
C11	**0.346724**	0.001177	
C12	0.126901	**0.410487**	
C13	**0.437300**	0.098703	
C14	0.000582	**0.390132**	
C15	**0.510705**	0.047918	
C16	0.000953	0.005388	
C17	0.001272	0.021411	
C18	0.000030	0.001402	
O1	0.000000	0.000002	
O2	0.000001	0.000015	
O3	0.000251	0.001117	
O4	0.000015	0.000300	
O5	0.000392	0.001893	
O6	0.000080	0.003693	
O7	**0.438479**	0.075333	
O8	0.088899	**0.401653**	

Element number are given as for Figure 1. The chemical forms of CA, DCA and ChA are shown as labeled in Figure 5. The chemical forms of RA are shown as CA partial form-DCA partial form; i.e. HA–AH and HA–HA forms are HA form of CA partial structure with AH form of DCA partial structure and HA form of CA partial structure with HA form of DCA partial structure, respectively.

those obtained from the ESR simulation, which indicate that the ChA and RA radicals are formed from the partial structures of CA and DCA, respectively. As in the case of CA, in ChA, the radical species derived from the (HA) form would be more preferentially detected by ESR than those derived from the (AH) form. Further, as in the case of DCA, the opposite would occur in the case of RA.

Spectral assignments of hyperfine coupling constants

Finally, we tried to assign the hfccs (Table I) obtained by ESR simulation to each hydrogen atom. The hydrogen atoms adjacent to an unpaired electron affect its hyperfine interaction in the order of distance [39]. Based on this principle, the hfccs are considered to be high near the radicalized regions, i.e. in the atoms with high HOMO values. For example, it is assumed that in the case of the (AH) form of CA, the hydrogen atom on C6 (Figure 7, assigned as the symbol ▩), that has the highest HOMO value, has the highest hfcc. Thus, the hfcc can be assigned to each hydrogen atom by referring to the HOMO values. In some cases, we need to consider the effect of all the chemical species present under the experimental conditions. In the case of CA, the characteristics of the two chemical species (AH) and (HA) should be considered; here, the contribution of the (HA) form to the hfcc is higher than that of the (AH) form due to the stability of the (HA) form as judged by the ease of ESR. Thus, we estimated the radicalized regions

referring to HOMO values and hfccs are assigned to each hydrogen atom, as shown in Figure 7.

In summary, we propose that in CA with an unsaturated side chain both monophenolate forms participate in the formation of the free radical species, while in DCA with a saturated side chain the diphenol form and both the monophenolate forms contribute to the formation of the free radical species, as analyzed by ESR and species distribution diagram. This proposal was partially supported by both molecular orbital calculations and ESR hyperfine coupling constants.

Our studies are now underway to examine the interaction of CA and its related compounds with DNA with respect to the DNA cleavage, which is promoted by the free radical forms of the polyphnols. The results will be reported.

References

[1] Al-Awwadi NA, Bornet A, Azay J, Araiz C, Delbosc S, Cristol J, Linck N, Cros G, Teissedre P. Red wine polyphenols alone or in association with ethanol prevent hypertension, cardiac hypertrophy, and production of reactive oxygen species in the insulin-resistant fructose-fed rat. J Agric Food Chem 2004; 52:5593–5597.

[2] Block G. The data support a role for antioxidants in reducing cancer risk. Nutr Rev 1992;50:207–213.

[3] Takeda H, Tsuji M, Miyamoto J, Matsumiya T. Rosmarinic acid and caffeic acid reduce the defensive freezing behavior of mice exposed to conditioned fear stress. Psychopharmacology 2002;164:233–235.

[4] Ito H, Miyazaki T, Ono M, Sakurai H. Antiallergic activities of rabdosiin and its related compounds: Chemical and biochemical evaluations. Bioorg Med Chem 1998;6:1051–1056.

[5] Hori M. Antioxidant and antiaging effect of evening primrose seed polyphenols. Frag J 2004;32:82–87.

[6] Pratt DE. Lipid antioxidants in plant tissue. J Food Sci 1965; 30:737–741.

[7] Pratt DE, Birac PM. Source of antioxidant activity of soybeans and soy products. J Food Sci 1979;44:1720–1722.

[8] Hudson BJF, Mahgoub SEO. Naturally-occurring antioxidants in leaf lipids. J Sci Food Agric 1980;31:646–650.

[9] Hayase F, Kato H. Antioxidative components of sweet potatoes. J Nutr Sci Vitaminol 1984;30:37–46.

[10] Cieślik E, Gręda A, Adamus W. Contents of polyphenols in fruit and vegetables. Food Chem 2006;94:135–142.

[11] Rice-Evans CA, Miller NJ, Paganga G. Structure–antioxidant activity relationships of flavonoids and phenolic acids. Free Radical Biol Med 1996;20:933–956.

[12] Nenadis N, Boyle S, Bakalbassis EG, Tsimidou M. An experimental approach to structure–activity relationships of caffeic and dihydrocaffeic acids and related monophenols. J Am Oil Chem Soc 2003;80:451–458.

[13] Leung J, Fenton TW, Clandinin DR. Phenolic components of sunflower flour. J Food Sci 1981;46(1386-1388):1393.

[14] Sotillo DRD, Hadley M, Holm ET. Phenolics in aqueous potato peel extract: Extraction, identification and degradation. J Food Sci 1994;59:649–651.

[15] Müller C, Hofmann T. Screening of raw coffee for thiol binding site precursors using "In bean" model roasting experiments. J Agric Food Chem 2005;53:2623–2629.

[16] Shahidi F, Wanasundara PKJPD. Phenolic antioxidants. Crit Rev Food Sci Nut 1992;32:67–103.

[17] Moon JH, Terao J. Antioxidant activity of caffeic acid and dihydrocaffeic acid in lard and human low-density lipoprotein. J Agric Food Chem 1998;46:5062–5065.

[18] Silva FAM, Borges F, Guimarães C, Lima JLFC, Matos C, Reis S. Phenolic acids and derivatives: Studies on the relationship among structure, radical scavenging activity, and physicochemical parameters. J Agric Food Chem 2000;48: 2122–2126.

[19] Bakalbassis EG, Nenadis N, Tsimidou M. A density functional theory study of structure–activity relationships in caffeic and dihydrocaffeic acids and related monophenols. J Am Oil Chem Soc 2003;80:459–466.

[20] Yamasaki H, Grace SC. EPR detection of phytophenoxyl radicals stabilized by zinc ions: Evidence for the redox coupling of plant phenolics with ascorbate in the H_2O_2-peroxidase system. FEBS Lett 1998;422:377–380.

[21] Li X, Cai Z, Katsumura Y, Wu G, Muroya Y. Reactions of reducing and oxidizing radicals with caffeic acid: A pulse radiolysis and theoretical study. Radiat Phys Chem 2001;60: 345–350.

[22] Namiki M, Yabuta G, Koizumi Y, Yano M. Development of free radical products during the greening reaction of caffeic acid esters (or chlorogenic acid) and a primary amino compound. Biosci Biotechnol Biochem 2001; 65: 2131–2136.

[23] Yoshioka H, Ohashi Y, Fukuda H, Senba Y, Yoshioka H. Spectral simulation of the ESR spectra of polyphenol radicals formed by reaction with hydroxyl radical. J Phys Chem A 2003;107:1127–1132.

[24] Hapiot P, Neudeck A, Pinson J, Fulcrand H, Neta P, Rolando C. Oxidation of caffeic acid and related hydroxycinnamic acids. J Electroanal Chem 1996;405:169–176.

[25] Atherton NM, Willder JSS. EPR and ENDOR of free radicals formed during the aerobic oxidation of chlorogenic acid and of caffeic acid in strongly alkaline solution. Res Chem Intermed 1993;19:787–795.

[26] Bors W, Michel C, Stettmaier K, Lu Y, Foo LY. Pulse radiolysis, electron paramagnetic resonance spectroscopy and theoretical calculations of caffeic acid oligomer radicals. Biochim Biophys Acta 2003;1620:97–107.

[27] Albert A, Serjeant EP. Ionization constants of acids and bases. A laboratory manual. London: Methuen; 1962.

[28] Schwarzenbach G. Metallokomplexe mit polyaminen I. Allgemeines. Helv Chim Acta 1950;33:947–962.

[29] Edsall JT, Martin RB, Hollingworth BR. Ionization of individual groups in dibasic acids, with application to the amino and hydroxyl groups of tyrosine. Proc Natl Acal Sci USA 1958;44:505–518.

[30] Ishimitsu T, Hirose S, Sakurai H. Microscopic acid dissociation constants of 3,4-dihydroxyphenylpropionic acid and related compounds, and 3,4-dihydroxyphenylalanine (DOPA). Talanta 1977;24:555–560.

[31] Ishimitsu T, Hirose S, Sakurai H. Microscopic acid dissociation constants of 3,4-dihydroxyphenethylamine (dopamine). Chem Pharm Bull 1978;26:74–78.

[32] Gao D, Kakuma M, Oka S, Sugino K, Sakurai H. Reaction of β-alkannin (shikonin) with reactive oxygen species: Detection of β-alkannin free radicals. Bioorg Med Chem 2000;8: 2561–2569.

[33] Stewart JJP. Optimization of parameters for semi-empirical methods II. Applications. J Comput Chem 1989; 10:221–264.

[34] Aoyama M, Kanno T, Ito O. Easy determination of polyphenol in plant sample by electron spin resonance Japan Kokai Tokkyo Koho 2004, JP 2004077266 A2 20040311 2004.

[35] Kiss T, Nagy G, Pécsi M. Complexes of 3,4-dihydroxyphenyl derivatives. X. Copper (II) complexes of chlorogenic acid and related compounds. Polyhedron 1989;8:2345–2349.

[36] Oess A, Cheshire MV, McPhail DB, Stoll S, Alaili ME, Vedy JC. Elucidation of phenol–Cu interaction mechanism by

potentiometry, ESR, UV absorption spectroscopy and molecular simulations. Sci Tot Environ 1999;228:49–58.

[37] Ishimitsu T, Hirose S, Sakurai H. Microscopic acid dissociation constants of 3,4-dihydroxyphenylbutyric acid and 3,4-dihydroxybenzoic acid. Chem Pharm Bull 1979;27: 247–251.

[38] Tanaka H, Sakurai H, Yokoyama A. Acid dissociation of selenocyteamine (2-aminoetheneselenol). Chem Pharm Bull 1970;18:1015–1020.

[39] Swartz HM, Bolton JR, Borg DC. Biological applications of electron spin resonance. New York, London, Sydney, Toronto: Wiley Interscience; 1972. p 33–38.